Eur. Phys. J. C (2008) 56: 323–332
DOI 10.1140/epjc/s10052-008-0679-2

THE EUROPEAN PHYSICAL JOURNAL C

Regular Article - Experimental Physics

Comparison of Geant4 hadron generation with data from the interactions with beryllium nuclei of +8.9 GeV/c protons and pions and −8.0 GeV/c pions

The HARP-CDP Group

A. Bolshakova[1], I. Boyko[1], G. Chelkov[1], D. Dedovitch[1], A. Elagin[1,2], M. Gostkin[1], A. Grishin[1], A. Guskov[1], Z. Kroumchtein[1], Yu. Nefedov[1], K. Nikolaev[1], A. Zhemchugov[1], F. Dydak[3], J. Wotschack[3,a], A. De Min[4,b], V. Ammosov[5], V. Gapienko[5], V. Koreshev[5], A. Semak[5], Yu. Sviridov[5], E. Usenko[5,6], V. Zaets[5]

[1]Joint Institute for Nuclear Research (JINR), Dubna, Russia
[2]*Present address:* Texas A&M University, College Station, USA
[3]CERN, Geneva, Switzerland
[4]Politecnico di Milano and INFN, Sezione di Milano-Bicocca, Milano, Italy
[5]Institute of High Energy Physics (IHEP), Protvino, Russia
[6]*Present address:* Institute for Nuclear Research RAS, Moscow, Russia

Received: 18 April 2008 / Revised: 24 June 2008 / Published online: 5 August 2008

Abstract Hadron generation in the Geant4 simulation tool kit is compared with inclusive spectra of secondary protons and pions from the interactions with beryllium nuclei of +8.9 GeV/c protons and pions, and of −8.0 GeV/c pions. The data were taken in 2002 at the CERN Proton Synchrotron with the HARP spectrometer. We report on significant disagreements between data and Monte Carlo simulation especially in the polar-angle distributions of secondary protons and pions.

PACS 13.75.Cs · 24.10.Lx

1 Introduction and motivation

The HARP experiment arose from the realization that the differential cross-sections of hadron production in the collisions of few GeV/c protons with nuclei were known only within a factor of two to three. Consequently, the HARP spectrometer was designed to carry out a programme of systematic and precise measurements of hadron production by protons and pions with momenta from 3 to 15 GeV/c. The experiment was in operation at the CERN Proton Synchrotron in 2001 and 2002, with a set of stationary targets ranging from hydrogen to lead, including beryllium.

The data from the HARP spectrometer can be used, amongst other purposes, for the physics validation of hadron generators that are used in simulation tool kits such as Geant4 [1, 2]. This is of interest for the correct interpretation of data that will be forthcoming, e.g., from experiments at the LHC [3].

In this paper, data are used from the HARP large-angle spectrometer that comprised a cylindrical Time Projection Chamber (TPC) and an array of Resistive Plate Chambers (RPCs) around the TPC. The purpose of the TPC was the measurement of the transverse momentum p_{T} and of the polar angle θ of tracks, and particle identification by $\mathrm{d}E/\mathrm{d}x$. The purpose of the RPCs was a complementary particle identification by time of flight.

The data analysis that underlies the spectra shown in this paper rests on the calibrations of the TPC and the RPCs that our group published in Refs. [4, 5]. For a more detailed account of our calibration work we refer to our collection of memos and analysis notes [6]. We recall that we disagree with the calibrations and physics results reported by the 'HARP Collaboration', as discussed in Refs. [7, 8].

With a view to correcting for losses of secondary particles from acceptance cuts, and for migration due to finite detector resolution, the measurement of tracks in the detector must be simulated with a Monte Carlo program. We use

[a] e-mail: joerg.wotschack@cern.ch
[b]On leave of absence at Ecole Polytechnique Fédérale, Lausanne, Switzerland.

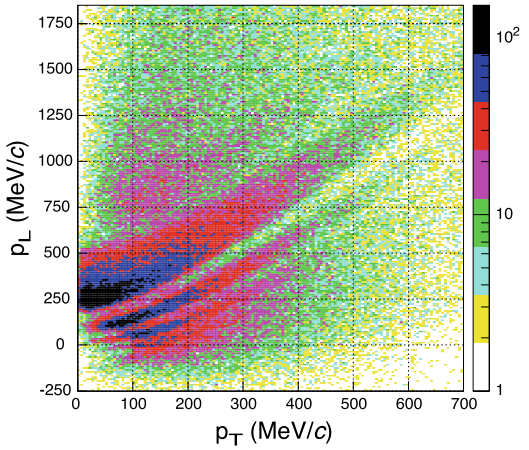

Fig. 1 Longitudinal momentum p_L versus transverse momentum p_T, as generated by Geant4's LHEP physics list for secondary π^+ from the interactions of $+8.9$ GeV/c beam π^+ with beryllium nuclei at rest

the Geant4 tool kit for this purpose. It was at this point that we noticed peculiar structures in the polar-angle spectra of secondary particles generated by Geant4's LHEP 'physics list' that prevented the weighting of generated tracks by smooth functions. Further investigations showed that this is a rather common phenomenon across Geant4's hadronic physics lists.

Figure 1 shows a typical example of a what we call unphysical structure. It shows the longitudinal momentum p_L versus transverse momentum p_T of secondaries as generated by Geant4's LHEP physics list. Since the structure, here clearly sticking out, is genuinely connected with the polar angle θ, it tends to be washed out when integrating over either p_L or p_T.[1] That may explain why—as nearly as we can tell—these structures were not noticed before.

2 Hadron generators in the Geant4 simulation tool kit

The Geant4 simulation tool kit provides several physics models of hadronic interactions of hadrons with nuclei, and collections of such models, termed physics lists. The latter are tailored with a view to optimizing performance for specific applications.

Table 1 lists and characterizes a representative selection of physics lists of hadronic interactions in Geant4,[2] together with the used physics models and the energy ranges where the latter are considered to be reliable [9].

In the so-called 'low-energy' domain (defined as kinetic energy E of the incoming hadron below some 25 GeV), a modified version of the GHEISHA package of Geant3 is used in many physics lists: the Parametrized Low-Energy Model ('LE_GHEISHA'). Optionally, for E below a few GeV, the Bertini Cascade [10] ('BERT') or the Binary Cascade [11] ('BIC') models can be enabled, with a view to simulating the cascading of final-state hadrons when they move through nuclear matter. As an alternative to LE_GHEISHA, a modified version of the FRITIOF string fragmentation model [12] ('FTF') is available.

In the so-called 'high-energy' domain, mostly the Quark–Gluon String Model ('QGSM') is used, with FTF and the Parametrized High-Energy Model ('HE_GHEISHA') as alternatives. Further terms that appear in Table 1 and are explained in Ref. [9], are 'PRECO' for the Pre-compound model, 'QEL' for the Quasi-elastic scattering model, and 'CHIPS' for the Chiral Invariant Phase Space model.

The energy ranges of models tend to overlap. In the overlap region, the model is chosen randomly but the choice is biased by the difference between the kinetic energy of the beam particle and the kinetic energy limits of the models.

Below, we compare the predictions of Geant4 hadronic physics lists with our data: the inclusive proton, π^+ and π^- spectra that are generated by the interactions with beryllium nuclei of $+8.9$ GeV/c protons and π^+, and of -8.0 GeV/c π^-.

3 The HARP large-angle spectrometer

3.1 Physics performance

For the purpose of this paper, the essential physics performance parameters are the resolution and the scale of the transverse momentum p_T of final-state particles, the resolution and the scale of the polar angle θ, and the separation of pions from protons. We briefly give evidence of the salient features, and refer the reader to our respective technical publications [4, 5] for details.

The resolution of the inverse transverse momentum measured by the TPC depends slightly on the relative velocity β and on θ of the particles. It is in the range $0.20 < \sigma(1/p_T) < 0.25$ $(\mathrm{GeV}/c)^{-1}$. Figure 2 shows the difference of the inverse transverse momentum of positive particles with $0.6 < \beta < 0.75$ and $45° < \theta < 65°$ from the measurement in the TPC and from the determination from RPC time of flight with the proton-mass hypothesis. The positive particles represent a nearly pure sample of protons, the background from pions and kaons is very small (the latter is demonstrated by the dots in Fig. 2 which stem from negative particles with the same selection cuts). Subtracting quadratically from the convoluted resolution of 0.27 $(\mathrm{GeV}/c)^{-1}$ the contribution from the time-of-flight resolution of the RPC, gives a net TPC resolution of $\sigma(1/p_T) = 0.20$ $(\mathrm{GeV}/c)^{-1}$.

[1] All physical quantities in this paper refer to the laboratory system.

[2] Version 9.1 dated 14 December, 2007.

Table 1 Overview of selected physics lists of hadronic interactions in Geant4

Physics list	Proton beam		$\pi^{\pm}$ beam	
LHEP	HE_GHEISHA	25 GeV–100 TeV	HE_GHEISHA	25 GeV–100 TeV
	LE_GHEISHA	0–55 GeV	LE_GHEISHA	0–55 GeV
LHEP_PRECO_HP	HE_GHEISHA	25 GeV–100 TeV	HE_GHEISHA	25 GeV–100 TeV
	LE_GHEISHA	0.15–55 GeV	LE_GHEISHA	0–55 GeV
	PRECO	0–0.17 GeV		
QGSC	QGSM+QEL+CHIPS	8 GeV–100 TeV	QGSM+QEL+CHIPS	8 GeV–100 TeV
	LE_GHEISHA	0–25 GeV	LE_GHEISHA	0–25 GeV
QGS_BIC	QGSM+BIC	12 GeV–100 TeV	QGSM+QEL	12 GeV–100 TeV
	LE_GHEISHA	9.5–25 GeV	LE_GHEISHA	1.2–25 GeV
	BIC	0–9.9 GeV	BIC	0–1.3 GeV
QGSP	QGSM+QEL+PRECO	8 GeV–100 TeV	QGSM+QEL+PRECO	8 GeV–100 TeV
	LE_GHEISHA	0–25 GeV	LE_GHEISHA	0–25 GeV
QGSP_BERT	QGSM+QEL+PRECO	8 GeV–100 TeV	QGSM+QEL+PRECO	8 GeV–100 TeV
	LE_GHEISHA	9.5–25 GeV	LE_GHEISHA	9.5–25 GeV
	BERT	0–9.9 GeV	BERT	0–9.9 GeV
QGSP_BIC	QGSM+QEL+PRECO	8 GeV–100 TeV	QGSM+QEL+PRECO	8 GeV–100 TeV
	LE_GHEISHA	9.5–25 GeV	LE_GHEISHA	0–25 GeV
	BIC	0–9.9 GeV		
QBBC	QGSM+QEL+CHIPS	6 GeV–100 TeV	QGSM+QEL+CHIPS	6 GeV–100 TeV
	BIC	0–9 GeV	BERT	0–9 GeV
FTFC	FTF+QEL+CHIPS	4 GeV–100 TeV	FTF+QEL+CHIPS	4 GeV–100 TeV
	LE_GHEISHA	0–5 GeV	LE_GHEISHA	0–5 GeV
FTFP	FTF	4 GeV–100 TeV	FTF+QEL+PRECO	4 GeV–100 TeV
	LE_GHEISHA	0–5 GeV	LE_GHEISHA	0–5 GeV
FTFP_BERT	FTF	4 GeV–100 TeV	FTF+QEL+PRECO	4 GeV–100 TeV
	BERT	0-5 GeV	BERT	0-5 GeV

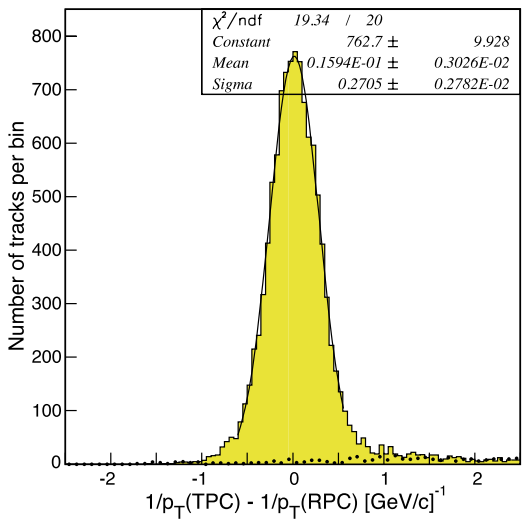

Fig. 2 Difference of the inverse transverse momenta of positive (*shaded histogram*) and negative (*black points*) particles from the measurement in the TPC and from the determination from RPC time of flight, for $0.6 < \beta < 0.75$ and for $45° < \theta < 65°$; the positive particles represent a nearly pure sample of protons; the background from pions and kaons is very small as demonstrated by the dots which show negative particles with the same selection cuts

From the requirement that π^+ and π^- with the same RPC time of flight have the same momentum, the momentum scale is determined to be correct to better than 2%, for both positively and negatively charged particles.

The polar angle θ is measured in the TPC with a resolution of $\sim$9 mrad, for a representative angle of $\theta = 60°$. To this a multiple scattering error has to be added which is $\sim$7 mrad for a proton with $p_T = 500$ MeV/c and $\theta = 60°$, and $\sim$4 mrad for a pion with the same characteristics. The polar-angle scale is correct to better than 2 mrad.

As for the separation of pions from protons: the resolution of dE/dx in the TPC is 16% for a track length of 300 mm, and the system time-of-flight resolution is 175 ps. Figure 3(a) shows the specific ionization dE/dx, measured by the TPC, and Fig. 3(b) the relative velocity β from the RPC time of flight, of positive and negative secondaries, as a function of the momentum measured in the TPC. The figures demonstrate that, in general, protons and pions are well separated. They also underline the importance of the complementary separation by RPC time of flight at large particle momentum. The average values of dE/dx and β agree well with theoretical expectations, thus confirming the validity of the absolute scales of momentum, dE/dx, and time of flight.

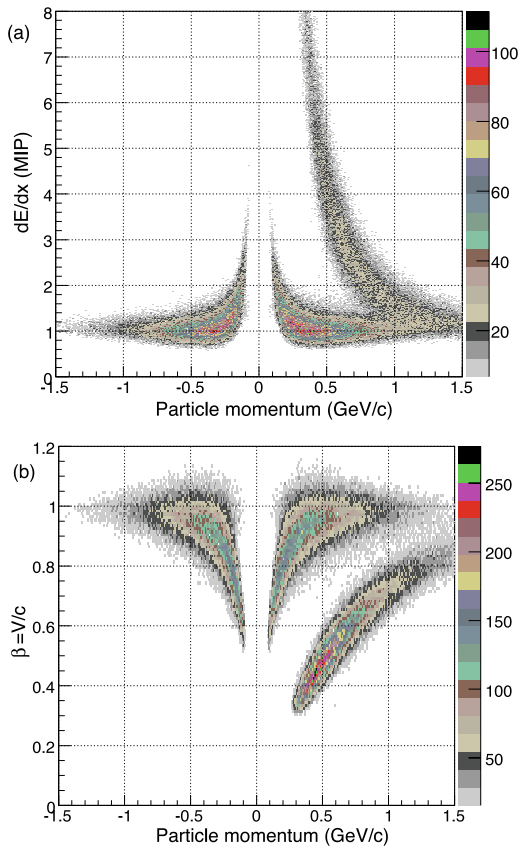

Fig. 3 Specific ionization $\mathrm{d}E/\mathrm{d}x$ [in units of minimum-ionizing pulse height] (**a**) and velocity β (**b**) versus momentum [GeV/c], for positive and negative tracks in $+8.9$ GeV/c data. The momentum sign reflects the particle charge

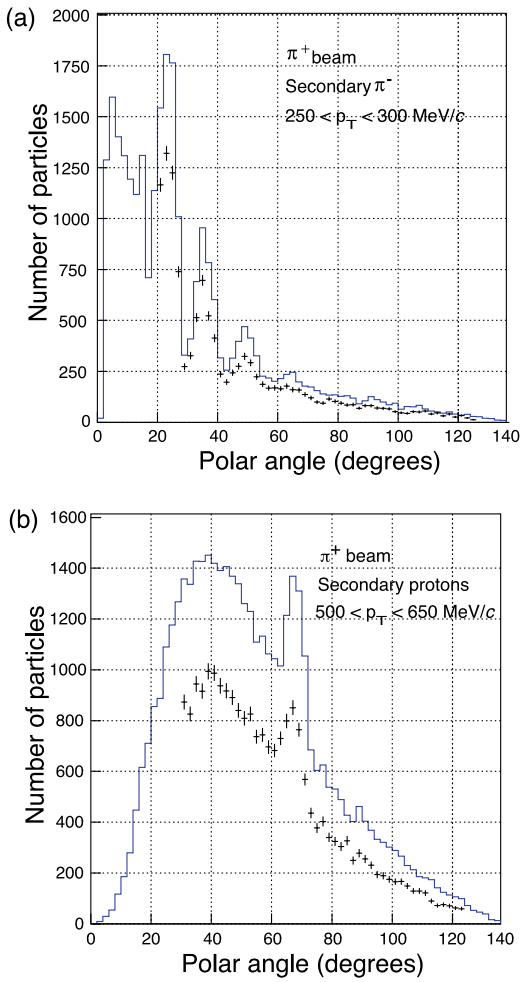

Fig. 4 Comparison of Monte Carlo generated (*full lines*) with Monte Carlo accepted (*crosses*) tracks; (**a**) polar-angle distributions of π^- for incoming π^+, and (**b**) of protons for incoming π^+

3.2 Acceptance and migration

We discuss differences of inclusive spectra between data and Monte Carlo simulation in terms of the distribution in the polar angle θ, for different ranges of p_T. The primary reason for this choice is that disagreements show up most clearly in θ. At the same time, θ is a well-measured experimental quantity. We also consider that the θ distribution provides the clue to the origin of the disagreements.

The physics performance parameters in the transverse momentum p_T and polar angle θ are so good that finite resolution, or a small dependence of acceptance cuts on p_T or θ, does not appreciably affect the comparison of data with Monte Carlo simulation (the chosen ranges of p_T exceed by a factor of two or more the p_T resolution, and the chosen bin size of 2° (35 mrad) of θ exceeds by a factor of two the θ resolution). That is substantiated in Figs. 4(a) and (b) for two polar-angle distributions showing rather striking disagreements between data and Monte Carlo simulation that will be discussed below in more detail. The full lines show the Monte Carlo generated polar-angle distributions, while the crosses show the same after acceptance cuts, particle identification cuts, and with resolution effects included. One concludes that the structures seen in the Monte Carlo simulation are not appreciably altered by experimental acceptance and resolution.

For the comparison of the shapes of inclusive particle spectra between data and Monte Carlo simulation—which is the purpose of this paper—it is, therefore, sufficient to compare data with Monte Carlo generated distributions, without correction of losses from acceptance cuts and of migration stemming from finite resolution. Also, the comparison is intentionally restricted to kinematical regions where there is ample and unambiguous separation of pions from protons.[3] To identify a secondary particle as a pion or as a proton it is required that the measured $\mathrm{d}E/\mathrm{d}x$ and time of

[3] Absolutely normalized double-differential cross-sections, obtained after due corrections for acceptance and migration, and making use of proper weights for particle identification and therefore spanning larger ranges of kinematical parameters than discussed in this paper, will be presented in forthcoming papers.

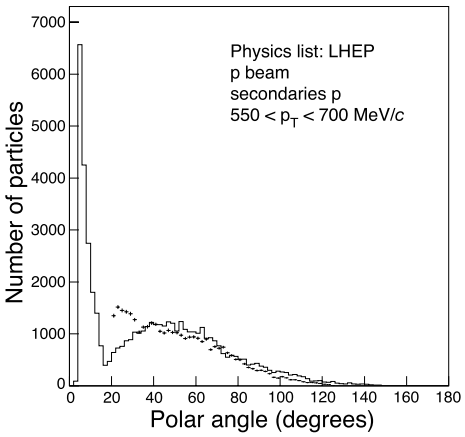

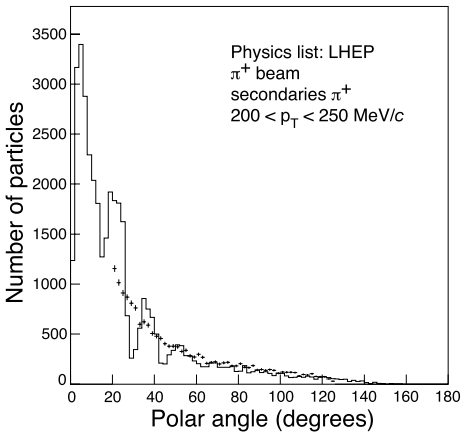

Fig. 5 LHEP physics list; polar-angle distributions of protons for incoming protons (*left panel*), and of π^+ for incoming π^+ (*right panel*); *full lines* denote the Geant4 simulation, *crosses* the data

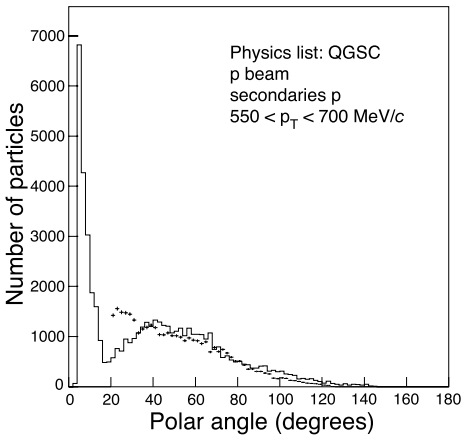

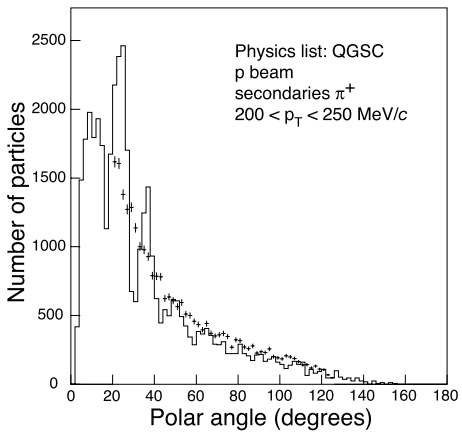

Fig. 6 QGSC physics list; polar-angle distributions of protons for incoming protons (*left panel*), and of π^+ for incoming protons (*right panel*); *full lines* denote the Geant4 simulation, *crosses* the data

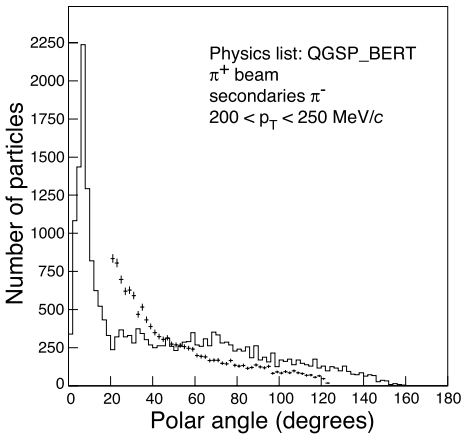

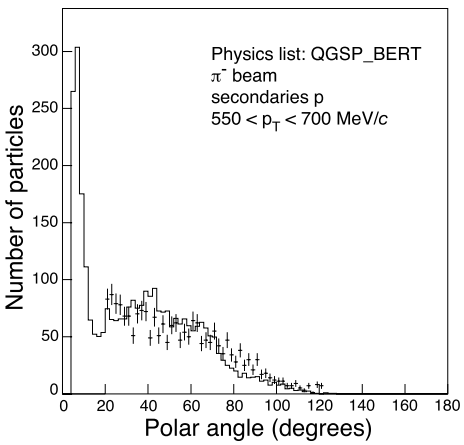

Fig. 7 QGSP_BERT physics list; polar-angle distributions of π^- for incoming π^+ (*left panel*), and of protons for incoming π^- (*right panel*); *full lines* denote the Geant4 simulation, *crosses* the data

flight are both consistent with the given particle hypothesis. In addition, the time of flight has to be inconsistent with the opposite hypothesis. For particles without either $\mathrm{d}E/\mathrm{d}x$ or time-of-flight measurement, the cut on the available variable is tightened. Within the accepted phase space, the particle identification efficiency is between 70% and 90%, while the contribution from wrong particle identification is below 5%.

4 Data versus simulation from selected Geant4 physics lists

The combination of the choice of hadron generators with the choice of incoming beam particles and the choice of secondary hadrons, leads to a large a number of possible plots. With a view to simplifying matters, we select for several physics lists two plots each that are representative for

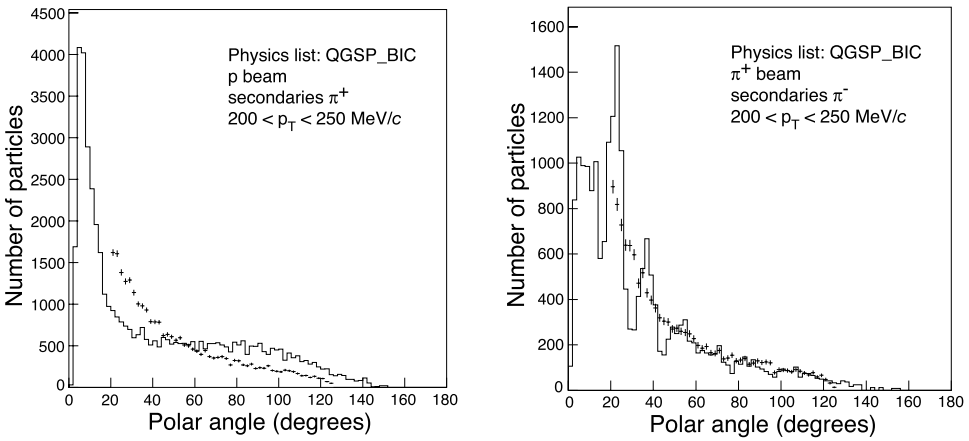

Fig. 8 QGSP_BIC physics list; polar-angle distributions of π^+ for incoming protons (*left panel*), and of π^- for incoming π^+ (*right panel*); *full lines* denote the Geant4 simulation, *crosses* the data

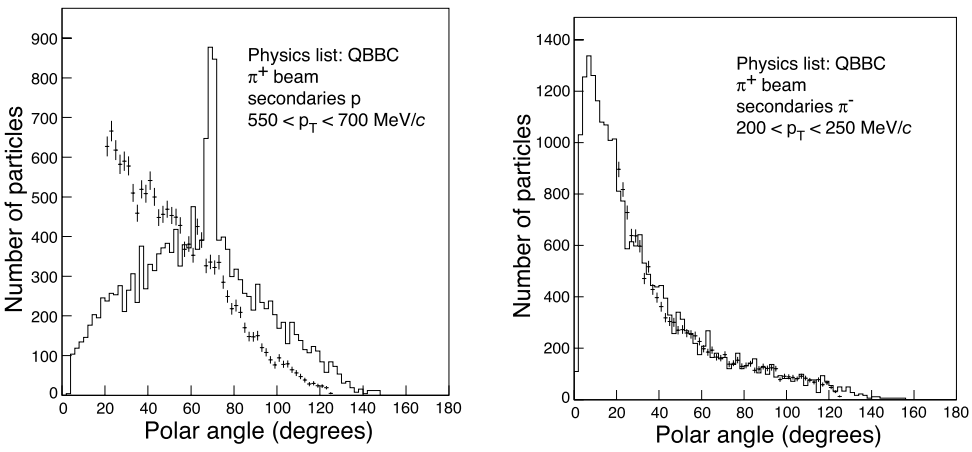

Fig. 9 QBBC physics list; polar-angle distributions of protons for incoming π^+ (*left panel*), and of π^- for incoming π^+ (*right panel*); *full lines* denote the Geant4 simulation, *crosses* the data

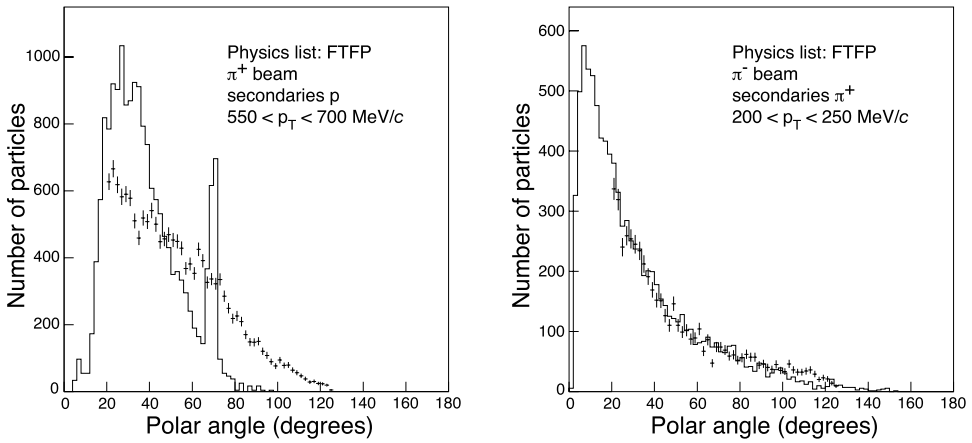

Fig. 10 FTFP physics list; polar-angle distributions of protons for incoming π^+ (*left panel*), and of π^+ for incoming π^- (*right panel*); *full lines* denote the Geant4 simulation, *crosses* the data

the agreement and disagreement, respectively, between data and simulation. They are shown in Figs. 5, 6, 7, 8, 9 and 10. We note that the LHEP physics list, while still an available option, is expected to become obsolete since it was intended to reproduce bulk calorimeter results only.

In all plots, we compare the Monte Carlo-generated θ distribution with the θ distribution of data. Positive beam particles have $+8.9$ GeV/c momentum, and negative beam particles have -8.0 GeV/c momentum. The target is a 5% λ_{abs} thick stationary beryllium target. Data are shown as crosses while Monte Carlo simulations are shown as full lines. As justified in Sect. 3.2, the data are not corrected for losses from acceptance cuts and migration stemming from finite resolution. With a view to emphasizing shape differences, the data are normalized to the Monte Carlo simulation in the angular range $20° < \theta < 125°$.

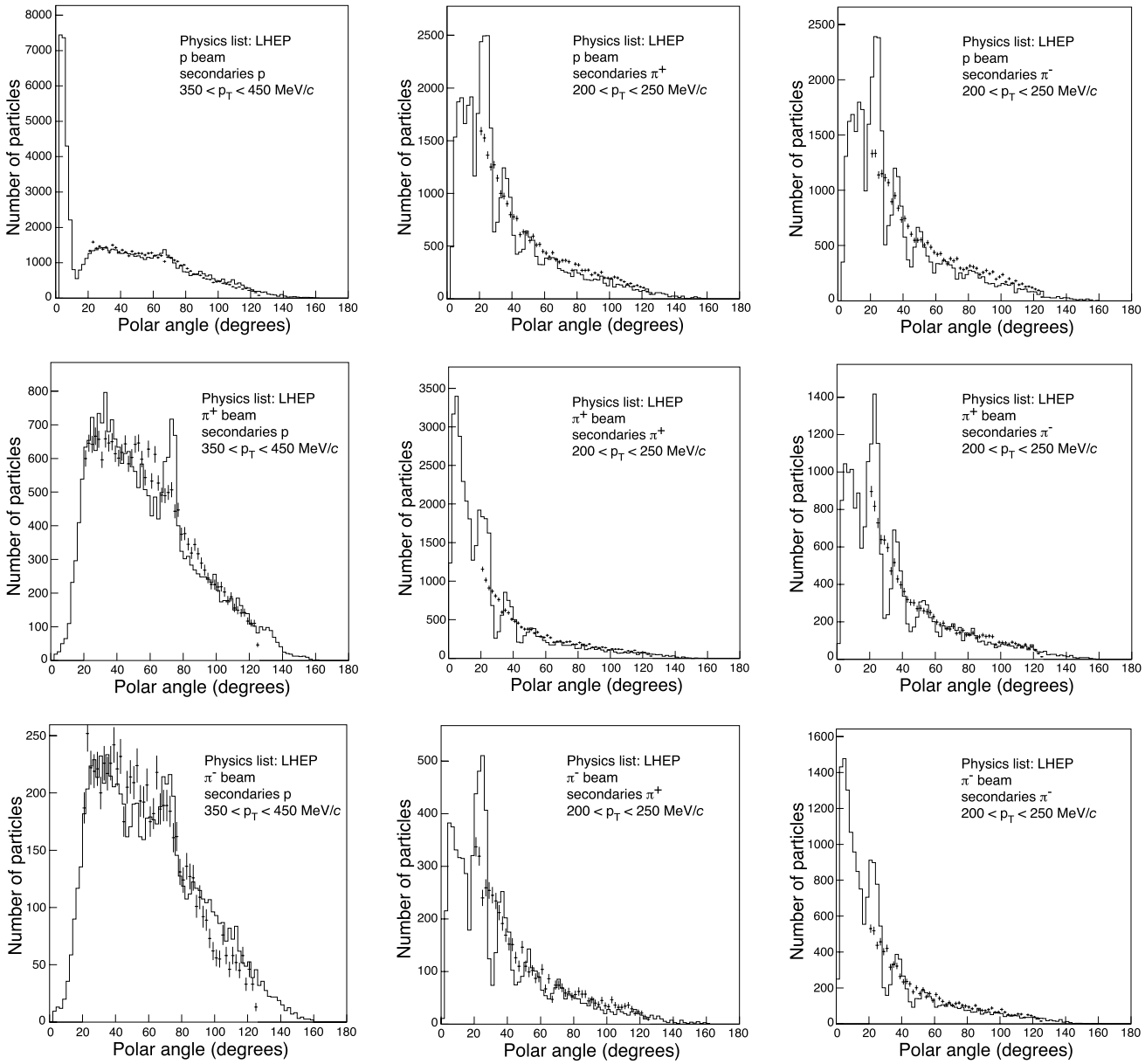

Fig. 11 LHEP physics list; polar-angle distributions of protons (*left panels*), π^+ (*middle panels*), and π^- (*right panels*), for incoming protons (*top row*), incoming π^+ (*middle row*), and incoming π^- (*bottom row*); *full lines* denote the Geant4 simulation, *crosses* the data

There are three distinct problems visible in the comparison of θ distributions of data and Monte Carlo simulation:

- a narrow peak for secondary protons near $\theta = 70°$;
- a diffraction-like pattern for secondary pions;
- a poor agreement in the shape.

The different physics lists behave differently with respect to the type of disagreement, yet the narrow peak for secondary protons near $\theta = 70°$, and the diffraction-like pattern for secondary pions appear as the most striking problems.

With a view to elucidating the origin of the latter, we examine more closely for the LHEP physics list the disagreements between data and Monte Carlo simulation for different combinations of incoming and secondary particle.

Figure 11 shows for a specific range of p_T all combinations of incoming and secondary protons, π^+ and π^-.

Figure 12 presents for the LHEP physics list in four ranges of p_T the spectra of secondary pions from incoming protons, and Fig. 13 the same for secondary protons from incoming pions.

The conclusions from the comparison of data with Monte Carlo simulation are summarized in Table 2. We qualify the various physics lists in the order 'good', 'acceptable', 'poor', 'unacceptable'. Our qualification is neither quan-

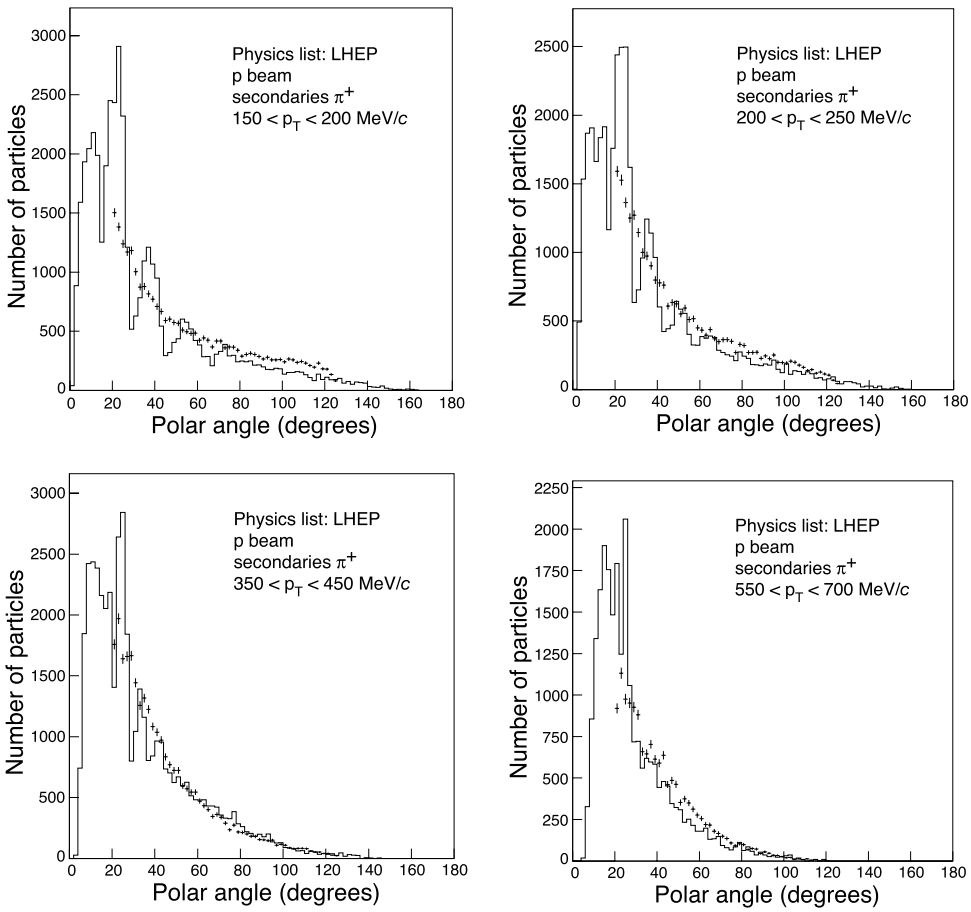

Fig. 12 LHEP physics list; polar-angle distributions of π^+, for incoming protons, in four different ranges of p_T; *full lines* denote the Geant4 simulation, *crosses* the data

titative nor entirely subjective: it is guided by the possibility to weight Monte Carlo distributions with smooth functions that require a few parameters only. Note that our qualification refers to the restricted polar-angle range $20° < \theta < 125°$.

We call a physics list 'good' if it reproduces the shape of the data without any need of adjustment, an example is the pion production by positive beam pions in the QBBC physics list as shown in Fig. 9(b). We call a physics list 'acceptable' if it reproduces more or less the shape of the data, but needs adjustments in some kinematical range, an example is the pion production by negative beam pions in the FTFP physics list as shown in Fig. 10(b). A physics list is called 'poor' if the shape of the Monte Carlo generated distribution is smooth but does not fit the data, examples are pion production by beam protons in the QGSP_BERT and QGSP_BIC physics lists as shown in Figs. 7(a) and 8(a). And finally, we call a physics list 'unacceptable' if the shape of the Monte Carlo generated distribution shows structures that cannot be removed by weighting with a smooth function, an example is pion production by beam protons in the QBBC physics list as shown in Fig. 9(a).

None of the standard physics lists of Geant4 is qualified 'good' or at least 'acceptable' in all channels.

The narrow peak in the distribution of secondary protons around 70° is consistent with the kinematics of elastic scattering of the incoming particle with a proton at rest. The diffraction-like pattern in the distribution of secondary pions is consistent with diffractive scattering of the incoming particle on a stationary disc with the diameter of a nucleon. We conjecture that the differences between data and Monte Carlo simulation arise from an inadequate description of the elastic scattering and diffraction scattering of incoming beam particles on nucleons embedded in a nucleus.

For the analysis of our data, we have used for incoming beam protons the QGSP_BIC physics list and see no strong reason to reconsider this choice. For incoming beam pions, none of the standard physics lists for hadronic interactions was acceptable, so we had to build our private HARP_CDP physics list. This physics list starts from the QBBC physics list (see Table 1). Yet the Quark–Gluon String Model is replaced by the FRITIOF string fragmentation model for kinetic energy $E > 6$ GeV; for $E < 6$ GeV, the Bertini Cascade is used for pions, and the Binary Cascade for protons; elastic and quasi-elastic scattering is disabled. Figure 14 shows the comparison of data with the simulation results from the HARP_CDP physics list. We qualify our

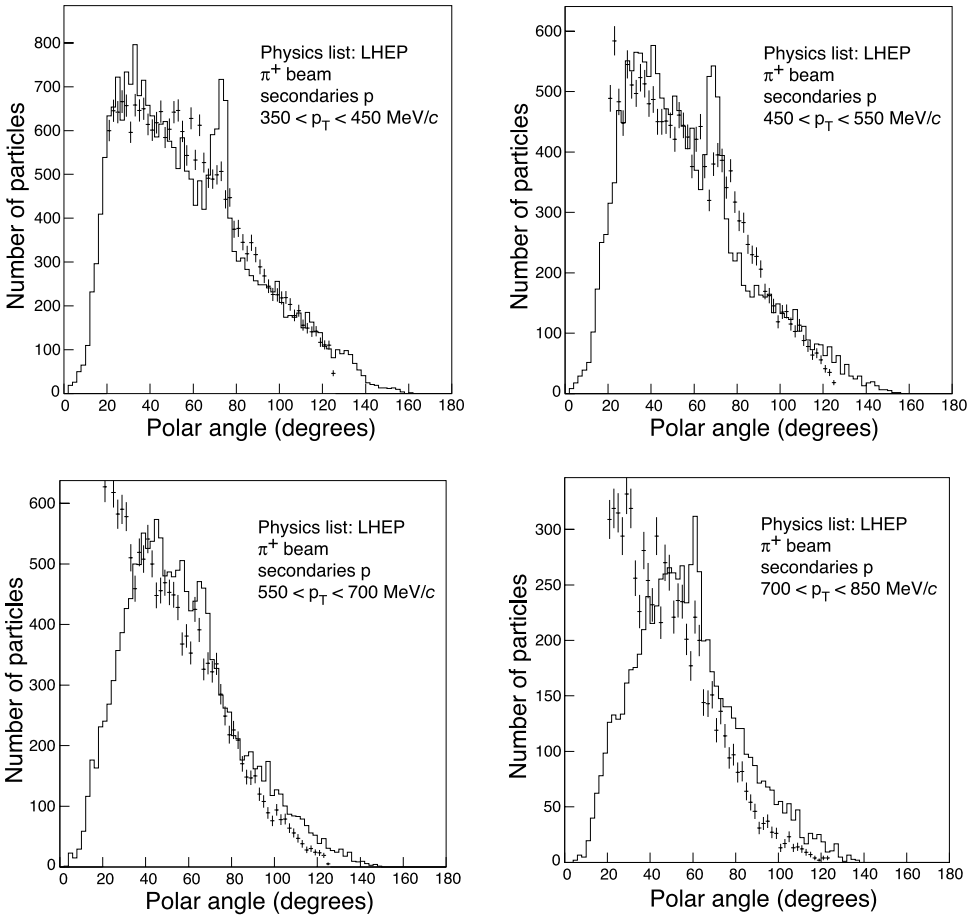

Fig. 13 LHEP physics list; polar-angle distributions of protons, for incoming π^+, in four different ranges of p_T; *full lines* denote the Geant4 simulation, *crosses* the data

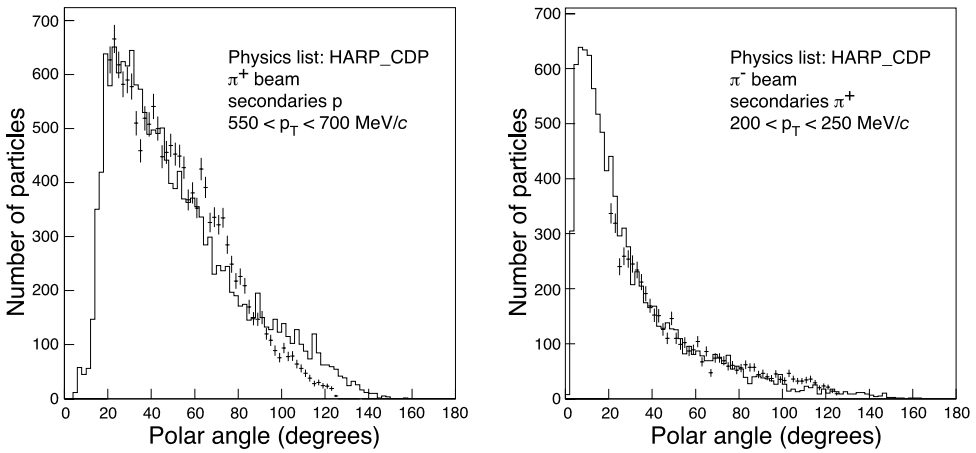

Fig. 14 HARP_CDP physics list; polar-angle distributions of protons for incoming π^+ (*left panel*), and of π^+ for incoming π^- (*right panel*); *full lines* denote the Geant4 simulation, *crosses* the data

HARP_CDP physics list as 'acceptable' in all four categories listed in Table 2.

5 Summary

We have presented significant disagreements in the laboratory polar-angle distributions between data from the HARP large-angle spectrometer, and results from the simulation by various physics lists in the Geant4 simulation tool kit. A narrow peak for secondary protons near $\theta = 70°$, and a diffraction-like pattern for secondary pions appear as most striking problems.

Acknowledgements We are indebted to J. Apostolakis, G. Folger, A. Ribon and D. Wright for a useful discussion on Geant4 intricacies. We are greatly indebted to many technical collaborators whose diligent and hard work made the HARP detector a well-working instrument. We thank all HARP colleagues who devoted time and effort to the design

Table 2 Conclusions on Geant4 standard physics lists of hadronic interactions

Physics list	Proton beam		$\pi^{\pm}$ beam	
	Secondary protons	Secondary $\pi^{\pm}$	Secondary protons	Secondary $\pi^{\pm}$
LHEP	**acceptable** (shape)	**unacceptable** (diffr. patt.)	**poor** (el. scatt. peak in π^+ beam)	**unacceptable** (diffr. patt.)
LHEP_PRECO_HP			**poor** (el. scatt. peak in π^+ beam)	**unacceptable** (diffr. patt.)
QGSC	**poor** (shape)	**unacceptable** (diffr. patt.)	**poor** (el. scatt. peak in π^+ beam)	**unacceptable** (diffr. patt.)
QGS_BIC			**poor** (el. scatt. peak in π^+ beam)	**unacceptable** (diffr. patt.)
QGSP	**poor** (shape)	**unacceptable** (diffr. patt.)	**poor** (el. scatt. peak in π^+ beam)	**unacceptable** (diffr. patt.)
QGSP_BERT	**poor** (shape)	**poor** (shape)	**acceptable** (el. scatt. peak in π^+ beam)	**poor** (shape)
QGSP_BIC	**poor** (shape)	**poor** (shape)	**poor** (el. scatt. peak in π^+ beam)	**unacceptable** (diffr. patt.)
QBBC	**unacceptable** (el. scatt. peak)	**acceptable**	**unacceptable** (el. scatt. peak)	**good**
FTFC			**unacceptable** (el. scatt. peak)	**acceptable**
FTFP	**unacceptable** (el. scatt. peak)	**poor** (shape)	**unacceptable** (el. scatt. peak)	**acceptable**
FTFP_BERT	**unacceptable** (el. scatt. peak)	**acceptable**	**unacceptable** (el. scatt. peak)	**acceptable**

and construction of the detector, to data taking, and to setting up the computing and software infrastructure. We express our sincere gratitude to HARP's funding agencies for their support.

References

1. S. Agostinelli et al., Nucl. Instrum. Methods Phys. Res. A **506**, 250 (2003)
2. J. Allison et al., IEEE Trans. Nucl. Sci. **53**, 270 (2006)
3. A. De Roeck et al., Preprint CERN-LCGAPP-2004-02
4. V. Ammosov et al., Nucl. Instrum. Methods Phys. Res. A **588**, 294 (2008)
5. V. Ammosov et al., Nucl. Instrum. Methods Phys. Res. A **578**, 119 (2007)
6. HARP-CDP bibliography. http://cern.ch/harp-cdp/HARP-CDP-bibliography.pdf
7. V. Ammosov et al., J. Instrum. **3**, P01002 (2008)
8. V. Ammosov et al., Eur. Phys. J. C **54**, 169 (2008)
9. Geant4 Physics Reference Manual. http://geant4.web.cern.ch/geant4/UserDocumentation/UsersGuides/PhysicsReferenceManual/fo/PhysicsReferenceManual.pdf
10. M.P. Guthrie, R.G. Alsmiller, H.W. Bertini, Nucl. Instrum. Methods **66**, 29 (1968)
11. G. Folger, V.N. Ivanchenko, J.P. Wellisch, Eur. Phys. J. A **21**, 407 (2004)
12. B. Andersson, G. Gustafson, B. Nielsson-Almqvist, Nucl. Phys. **281**, 289 (1987)